Observed and modelled multi-frequency sea ice covariability

Molly M. Wieringa[1] & Cecilia M. Bitz[1]

[1]*University of Washington, Department of Atmospheric Sciences, Seattle WA, USA*

Preliminary results suggest that spatial patterns of sea ice variability evolve across timescales and that while there is good agreement on sea ice concentration variability, observations and models capture sea ice thickness variability differently.

Introduction

This study seeks to incorporate information about sea ice thickness (SIT) into various analyses of sea ice variability, as SIT is a crucial determinant of sea ice "memory" [*1*], but is subject to dynamic forces on shorter timescales. As continuous SIT observations are relatively new, this studies also seeks to compare observed SIT variability to its modelled counterparts.

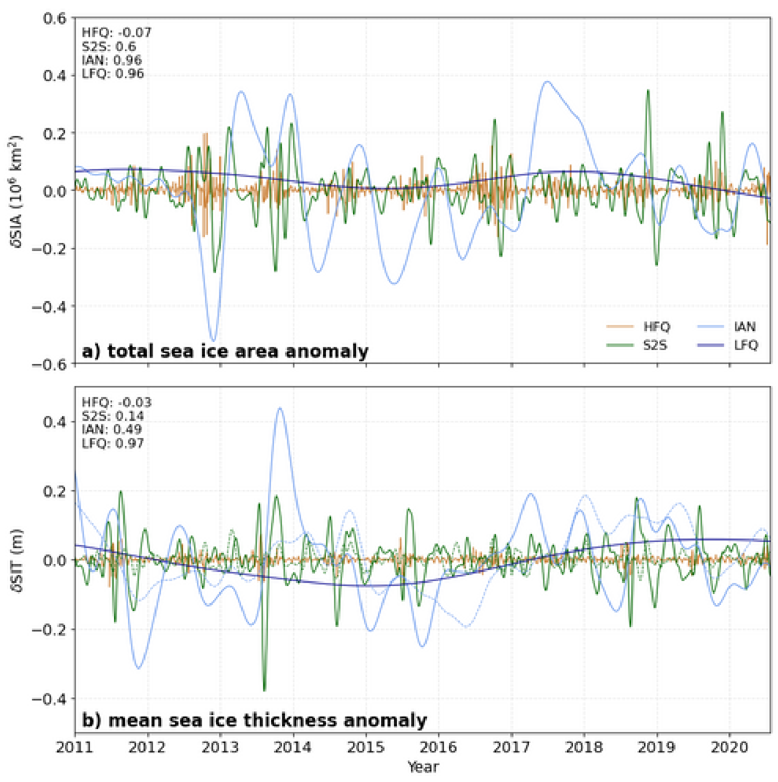

Figure 1. Total Arctic SIA anomalies **(a)** and mean Arctic SIT anomalies **(b)** from PIOMAS, filtered into HFQ, S2S, IAN, and LFQ timescales (*see Data & Methods*), are plotted in solid lines. Cryosat-2 SIT anomalies are plotted in dotted lines for S2S and IAN timescales as they differ notably from PIOMAS. Correlation coefficients between PIOMAS and Cryosat-2 at each timescale are listed in the upper left corner.

Data & Methods

Daily **SIC and SIT data derived from Cryosat-2** [*2*] is compared to the **PIOMAS sea ice reconstruction** [*3*] and analyzed relative to daily atmospheric variables **(SST, SLP, U10, V10, and Z500) from the ERA5 reanalysis** [*4*]. All data are trimmed to the 2011-2020 time period and regridded to a rectilinear 1x1 degree grid.

Timeseries Filtering

Butterworth filter applied to daily SIC and SIT anomalies from Cryosat-2 and PIOMAS

- high-frequency (**HFQ**): <10 days
- seas. to subseas. (**S2S**): 10 days - 6 mo
- interannual (**IAN**): 6 mo - 18 mo
- low-frequency (**LFQ**): > 18mo

Frequency Component Analysis

Adapted from [*5*] to filter HFQ, S2S, IAN, & LFQ

- Find *combinations of the data's leading EOF patterns that explain the maximum amount of the data's filtered covariance*
- Regress frequency components (FC) onto ERA5 variables to explore drivers of each frequency pattern (FP).

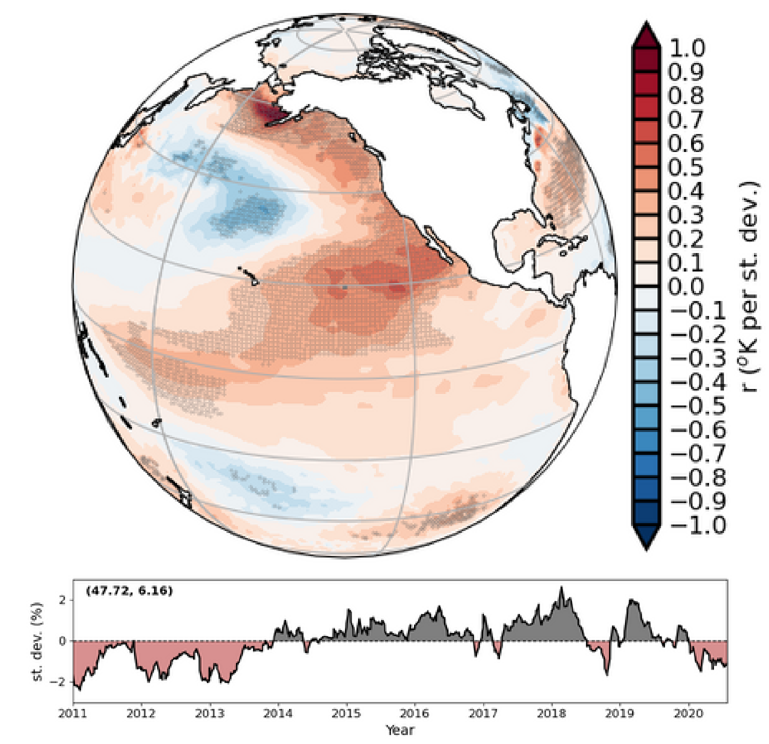

Figure 2. Sea surface temperature anomaly pattern associated with the leading LFQ mode of the Cryosat-2 sea ice data (*top*) and the associated frequency component (FC) (*bottom*), which accounts for 47.72% of the LFQ variance and 6.16% of the total variance. Gray stippling indicates points where the regression between SST and the leading FC has R^2 > 0.15.

Reconstruction vs. Observations

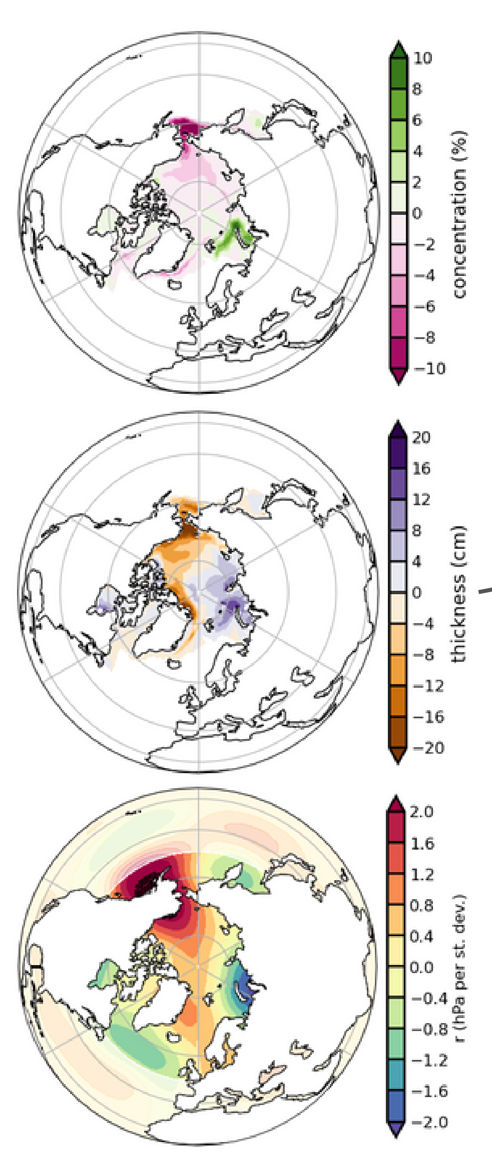

Figure 4. The FCA leading mode patterns of PIOMAS SIC (*top*) and SIT (*middle*) on the S2S timescale. The Z500 geopotential height anomaly pattern associated with this mode is also shown (bottom, *0-55N faded for visualization*).

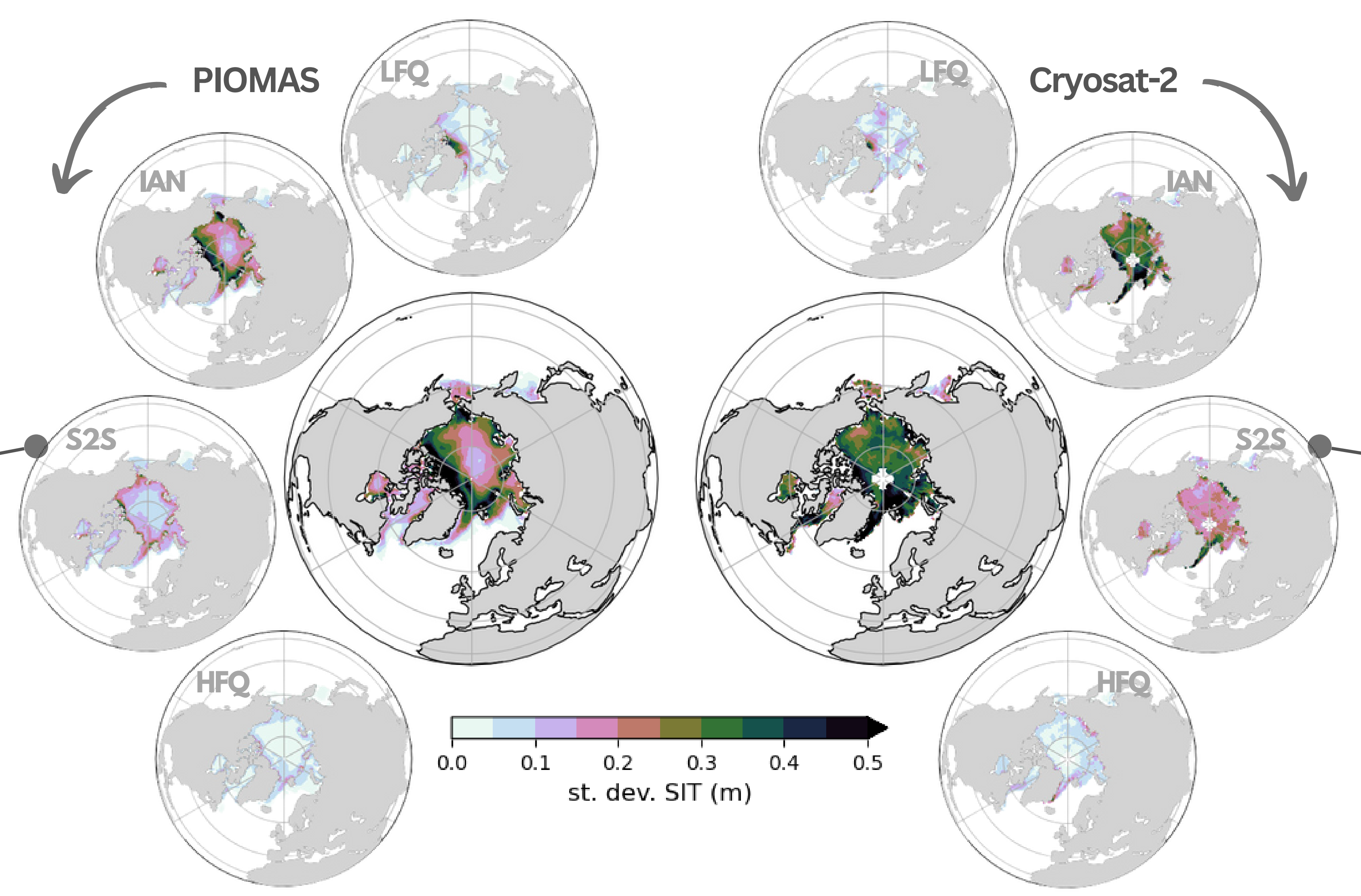

Figure 3. Sea ice thickness variability, estimated as the standard deviation of SIT anomalies for unfiltered PIOMAS (center left) and Cryosat-2 (center right) data. Corresponding estimates of SIT variability on high frequency (HFQ), seasonal-to-subseasonal (S2S), interannual (IAN), and low frequency (LFQ) filtered timescales are also shown in ascending order for each product.

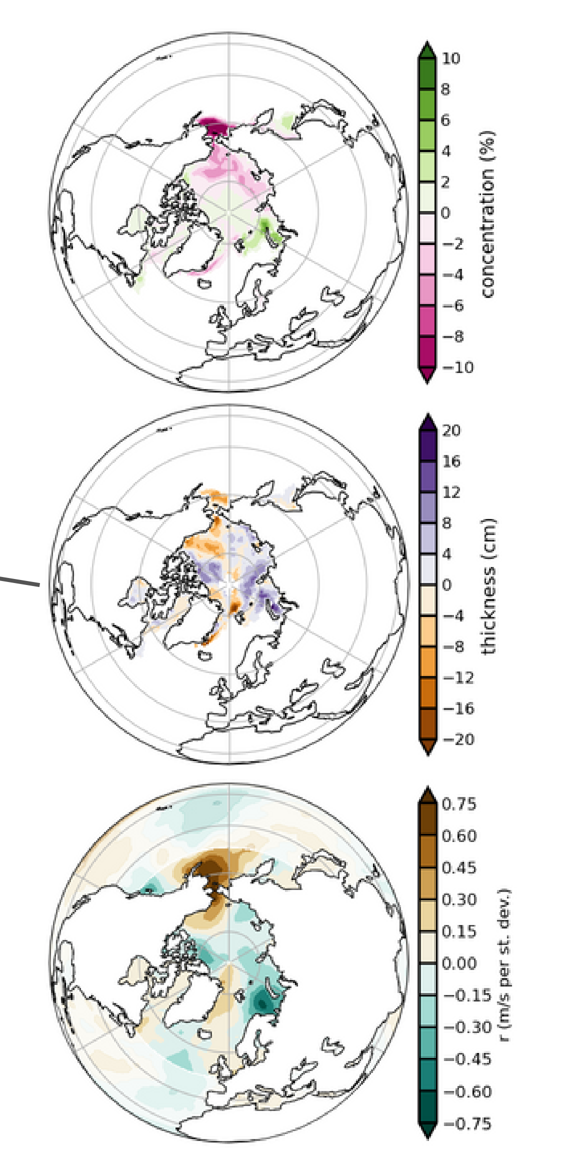

Figure 5. The FCA leading mode patterns of Cryosat-2 SIC (*top*) and SIT (*middle*) on the S2S timescale. The 10-meter meridional wind anomaly pattern associated with this mode is also shown (bottom, *0-55N faded for visualization*).

Climate Models

Initial comparison of observational anomalies to model large ensembles indicates issues with SIT.

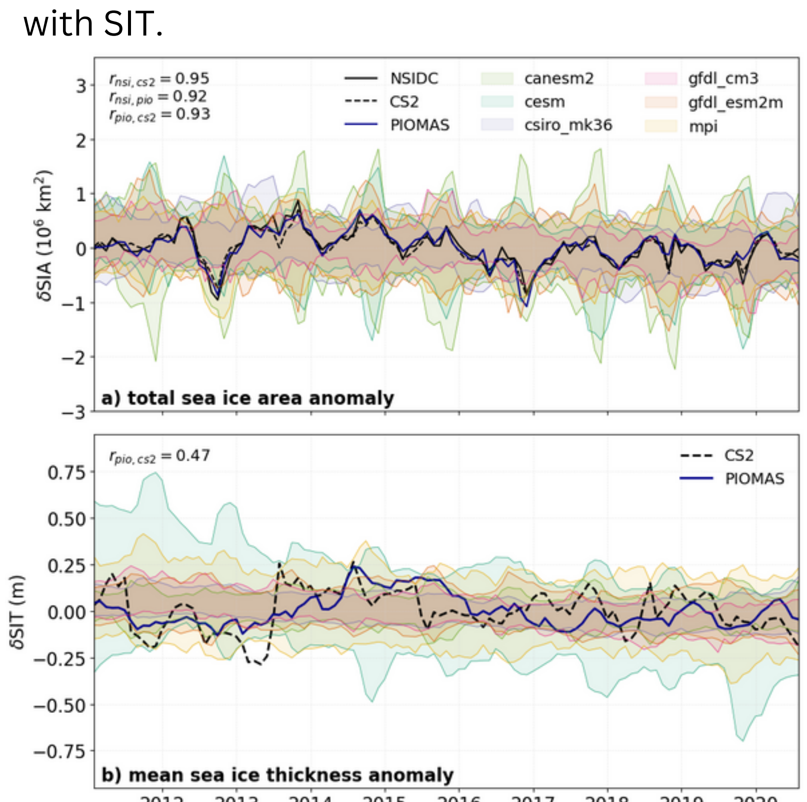

Figure 6. Total Arctic SIA anomalies **(a)** and mean Arctic SIT anomalies **(b)** from observational products (solid and dashed lines) and 6 GCM Large Ensembles [*11*] (colored shading). Each model envelope is calculated by taking the maximum and minimum values across ensemble members. All data was centered and deseasonalized, but retains a forced response.

Discussion

While many of the results shown here are preliminary and have largely targeted S2S and LFQ timescales, the following observations are noteworthy:

1. The leading LFQ frequency pattern and its associated SST pattern (Fig. 2) is reminiscient of the Pacific-Arctic teleconnection (PARC) identified in previous literature [*6*].
2. Patterns of SIT variability differ notably between Cryosat-2 and PIOMAS, particularly on S2S and IAN timescales (Figs. 1 and 3, *note sampling bias for LFQ in this work*). This influences each product's leading S2S frequency pattern for SIT (though both products' leading FC captures ~15% of the S2S covariance). In PIOMAS, the SIT pattern tracks the regressed Z500 anomaly pattern, suggesting a **thermodynamic** control; in Cryosat-2, the leading SIT FP corresponds more directly with the V10 anomaly pattern, potentially capturing a more **dynamic** driver.
3. Observational products agree quite well on SIC variability (*r > 0.9*, Fig. 6) but comparatively poorly on SIT variability (*r < 0.5*, Fig. 6). SIC variability (including the forced trend) is also better capture by model large ensembles than SIT variability.

Finally, we have explored removing the forced response from each sea ice dataset in this short observational period by removing (a) linear trends; (b) quadratic trends; and (c) the leading LFQ SIC-SIT-SST mode [*7, 8*] and found little or inconclusive impact.

Ongoing Work

Current and future avenues for this project:

- A robust metric of significance for the FCA is still required
- Explore the use of an ML algorithm to removed the forced response from observations [*9*].
- Explore the grid cell variability of SIC and SIT, where covariability may be limited when SIC approaches 100% (Fig. 7)
- Seasonal analysis within the FCA

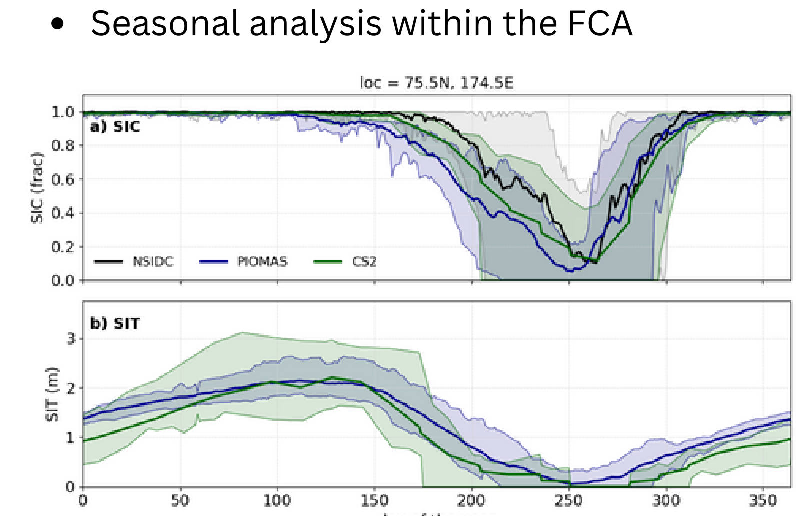

Figure 7. Daily sea ice variability in SIC **(a)** and SIT **(b)** at a single grid cell in the Arctic, represented as an "observed ensemble" of data from years 2011-2020 (*each year = 1 ensemble member*). The shaded envelope is determined as in Fig. 6, and bold lines represented the "ensemble" mean.

References

1. Blanchard-Wrigglesworth et al. (2011), *J. Clim.*; **2**. Landy et al. (2022), *Nature*; **3**. Schweiger et al. (2011), *J. Geophys. Res.*; **4**. Hersbach et al. (2020), *Q.J.R. Meteorol. Soc.*; **5**. Wills et al. (2018), *Geo. Res. Lett.*; **6**. Baxter et al. (2019), *J. Clim.*; **7**. Dörr et al. (2023), *Cryosphere*; **8**. Bonan et al. (2023, *preprint*), *Cryosphere*; **9**. Sweeney et al. (2023), *Geo. Res. Lett.* **10.** Meier et al. (2011), *NSIDC.* **11**. Deser et al. (2020), *Nat. Clim. Change.*

Acknowledgements: *the authors thank Ed Blanchard-Wrigglesworth, David Bonan, and Aodhan Sweeney for helpful conversations that have shaped this project and acknowledge that the majority of the work has been conducted on the unceded lands of the Coast Salish and Duwamish people, past and present.*